stresses

MDPI

Article

Cocoa Apoplastic Washing Fluid Remodels the Proteomic Profile of the Saprophytic Mycelium of *Moniliophthora perniciosa*, the Causal Agent of Witches' Broom Disease

Luciana Rodrigues Camillo [1], Ariana Silva Santos [2,*], Irma Yuliana Mora Ocampo [3], Edson Mario de Andrade Silva [4], Fátima Cerqueira Alvim [3], Karina Peres Gramacho [5] and Carlos Priminho Pirovani [3]

[1] Instituto Agronômico de Campinas, Centro de Citricultura Sylvio Moreira—IAC/CCSM, Rodovia Anhanguera, km 158, Cascalho Cordeirópolis 13020-902, São Paulo, Brazil; lurcam@gmail.com
[2] Colegiado de Ciências da Natureza, Campus Senhor do Bonfim, Universidade Federal do Vale do São Francisco, Senhor do Bonfim 48970-000, Bahia, Brazil
[3] Departamento de Biologia, Centro de Genética e Biologia Molecular, Universidade Estadual de Santa Cruz, Campus Soane Nazaré de Andrade, Rodovia Jorge Amado, Ilhéus 45662-900, Bahia, Brazil; yulimoraocampo@gmail.com (I.Y.M.O.); alvim@uesc.br (F.C.A.); pirovani@uesc.br (C.P.P.)
[4] Horticultural Sciences Department, University of Florida, Gainesville, FL 32611, USA; mariodeandradee@gmail.com
[5] Centro de Pesquisa do Cacau—CEPEC/CEPLAC, Departamento de Fitopatologia, Ilhéus 45600-000, Bahia, Brazil; karinagramacho@gmail.com
* Correspondence: ariana.ssantos@univasf.edu.br; Tel.: +55-75-992404131

Abstract

Witches' broom disease (WBD), caused by the fungus *Moniliophthora perniciosa*, poses a major threat to cocoa production and little is yet known about how the fungus adapts at the molecular level, particularly in the apoplastic environment during early infection. Here, we investigated how apoplastic washing fluid (AWF) from two cocoa genotypes with contrasting resistance to WBD modulates the mycelial protein profile of two *M. perniciosa* isolates: (i) Mp553—low infection level; and (ii) Mp565—high infection level. A total of 1272 proteins were identified. Mp565, showed increased accumulation of proteins associated with oxidative stress response, energy metabolism, and virulence when exposed to AWF from the resistant variety TSH1188. Key proteins such as phosphoglycerate kinase, enolase, and heat shock were significantly modulated. Interestingly, AWF from the resistant variety promoted the suppression of metabolic proteins, suggesting an effective defense response in the resistant genotype. Furthermore, interaction network analysis revealed the central role of the MPER_11800 protein, a potential regulator of fungal adaptation. The findings underscore the importance of the *T. cacao* apoplast in both plant defense and fungal adaptation. The study also reveals key molecular targets, such as MPER_11800, for potential strategies to control WBD. These insights enhance our understanding of *M. perniciosa* pathogenicity and offer valuable directions for developing novel interventions to mitigate the impact of this devastating disease.

Keywords: apoplastic washing fluid; apoplastome; *Moniliophthora perniciosa*; *Theobroma cacao*

Academic Editor: Yasutomo Hoshika

Received: 15 April 2026
Revised: 20 May 2026
Accepted: 26 May 2026
Published: 1 June 2026

1. Introduction

Moniliophthora perniciosa is the causal agent of one of the most severe diseases of *Theobroma cacao* L.—witches' broom disease (WBD), a dynamic and complex pathosystem.

Global cocoa bean production reached approximately 4.38 million tons in the 2023/24 season, driven by favorable weather conditions. For the 2025/2026 period, the harvest is estimated at approximately 4.7 to 4.9 million tons, according to data and projections from the International Cocoa Organization (ICCO), indicating a recovery in global supply and a possible return to a surplus scenario after years of deficit, especially in the 2023/2024 harvest [1,2]. This is a reflection of climate problems faced by the world's main producers, such as irregular rainfall patterns and increased humidity, which aggravate the incidence of fungal diseases, such as WBD [3].

Theobroma cacao L. has great socioeconomic importance, and cocoa-derived products also contribute to human health by inducing modulations in the human antioxidant system, as well as promoting secondary metabolites that accumulate in regions of the cerebral cortex responsible for memory and learning [4,5].

Moniliophthora perniciosa, a hemibiotrophic fungus, has a peculiar life cycle in comparison with other hemibiotrophic fungi. This life cycle consists of two phases: (i) biotrophic, initial phase of colonization of plant tissue, where the mycelium grows intercellularly; and (ii) necrotrophic, involving the development of dikaryotic hyphae and connecting clamps, giving rise to necrotic symptoms typical of WBD [6–8]. In the biotrophic phase, *M. perniciosa* remains in the extracellular space, the apoplast, for about 40 to 60 days until progressing to the saprophytic phase [9,10]. Additionally, Ceita et al. [10] reported the simultaneous presence of mono- and dikaryotic hyphae within the infected leaf tissue of *T. cacao* during the transition between the biotrophic and necrotrophic phases. This description reveals that even in the phase characterized as biotrophic, dikaryotic hyphae typical of saprophytic mycelium can be observed in the apoplast (Figure 1).

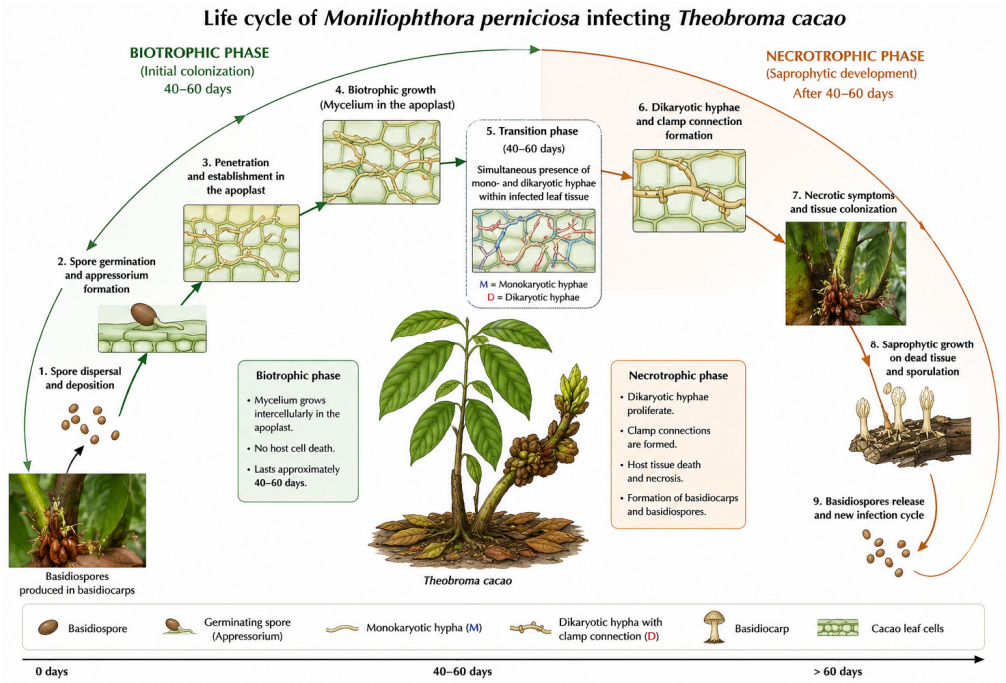

Figure 1. Schematic representation of the life cycle of *Moniliophthora perniciosa* infecting *Theobroma cacao*, highlighting the biotrophic and necrotrophic phases of witches' broom disease development. Figure created with AI-assisted illustration tools (OpenAI ChatGPT/DALL·E 5.5) using author-defined scientific prompts.

Many reactions that are of great importance to the plant occur in the host's apoplast space, such as nutrient and water transport, synthesis of cell wall components, synthesis of proteins such as the PR family (related to pathogenesis) and phytoalexins involved in plant defense against biotic and abiotic stresses, since environmental changes are initially

detected in the apoplast [11,12]. Thus, the apoplast can be considered the first barrier between the cell and the surrounding environment.

In situations of biotic stress, pathogen control can occur in the apoplast, based on changes in nutrient composition and metabolism. Furthermore, this defense mechanism in response to the presence of the pathogen includes production of reactive oxygen species (ROS), toxic compounds and protein molecules with antipathogenic activity, such as PR, in addition to effector proteins, peptides and small molecules secreted into the apoplastic space [13–16].

Thus, the molecular modulation of the apoplast in the plant–pathogen interaction has become the target of many studies, to understand the mechanisms of pathogen infection regarding the response actions of the plant whose development is compromised [16–20]. Proteomic studies have also contributed in this regard. Recently, the first apoplastic proteomic profile of contrasting genotypes in relation to *T. cacao* resistance to WBD was reported [16]. Proteins such as peroxidases, chitinases and osmotin were modulated in the apoplastome of *T. cacao*. Furthermore, the efficiency of apoplastic washing fluid (AWF) from *T. cacao* genotypes in inhibiting *M. perniciosa* spore germination was demonstrated.

Also investigating the apoplastome of *T. cacao* genotypes regarding resistance to WBD, Oliveira et al. [17] identified an arsenal of pathogenesis-related proteins (PR): PR-2 (β-1,3-glucanases), PR-3 and PR-4 (chitinases), PR-5 (thaumatin), PR-9 (peroxidases) and PR-14 (lipid transfer proteins), as well as proteins from microorganisms in the AWF. These results confirm that the apoplast is fundamental in the complex *T. cacao* × *M. perniciosa* pathosystem. Therefore, it can be stated that the apoplast of *T. cacao* can provide important responses during the interaction with *M. perniciosa*.

Therefore, the protein modulation of the fungus in the apoplast of *T. cacao* has not yet been clarified, especially regarding the differential expression of proteins involved in the phase of greatest development of the fungus—the mycelial stage. Accordingly, to advance understanding of the protein profile underlying WBD induced by the fungus *M. perniciosa*, here we report the modulation of the mycelial protein profile of two isolates of the fungus *M. perniciosa* elicited with apoplastic washing fluid (AWF) from cocoa varieties contrasting in their resistance to WBD.

2. Results

2.1. Dikaryotic Mycelium Profile of Isolates Mp553 and Mp565 in Cultivation with Cocoa AWF

The protein profiles of isolates Mp553 and Mp565 grown in the presence of AWF from Catongo (susceptible) and TSH1188 (resistant) showed predominantly similar banding patterns, with well-resolved proteins, mainly distributed between 14 and 97 kDa. Differential band intensities were more evident in the 45–66 kDa range, particularly in Mp565 compared to Mp553, although subtle differences were also observed between 30 and 45 kDa (Supplementary Figure S1). Proteins above 97 kDa showed lower resolution under the electrophoretic conditions employed. Differences in the protein profile of the mycelia of each isolate, under the control conditions (Ctrl—without AWF) and treated with Cat AWF and TSH, are shown in the two-dimensional gels (Supplementary Figure S2). In comparison with the Ctrl condition, there was an accumulation of proteins in the different treatments for the isolates, mainly in the Mp553 isolate grown in Cat AWF and TSH.

A total of 1272 spots were detected for isolates Mp553 and Mp565 in the different treatments (Ctrl, Cat and THS). There were 755 spots for isolate Mp553 and 517 spots for isolate Mp565 (Figure 2). Of these, 452 were in common between the AWF treatments to which isolate Mp553 was subjected, while 301 were common to Mp565.

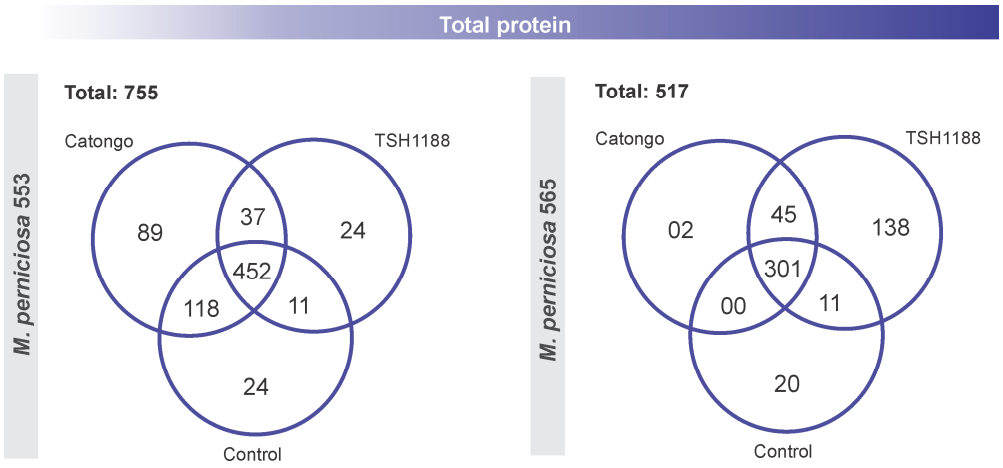

Figure 2. Total number of spots detected in *Moniliophthora perniciosa* isolates Mp553 and Mp565, in response to AWF of the genotypes *T. cacao*, Catongo, TSH1188 and the control condition (No AWF).

In Mp553, 89 unique protein spots were detected in response to AWF from the susceptible genotype, Catongo, in contrast to the same genotype, having only two spots for the more aggressive isolate Mp565. In the treatment with AWF from TSH, a resistant genotype, 24 unique spots were detected in the isolate Mp553 and 138 spots in Mp565 (Figure 2).

2.2. Protein Mapping and Identification by LC-MS/MS

Reference maps were generated for Mp553 and Mp565 to compare the proteomic profiles of the isolates under controlled conditions and after exposure to AWF from contrasting cacao genotypes (Figure 3A,B). Differentially accumulated spots were determined based on intensity variation ($p \leq 0.05$; fold change ≥ 1.5) and are highlighted in red in Figure 3.

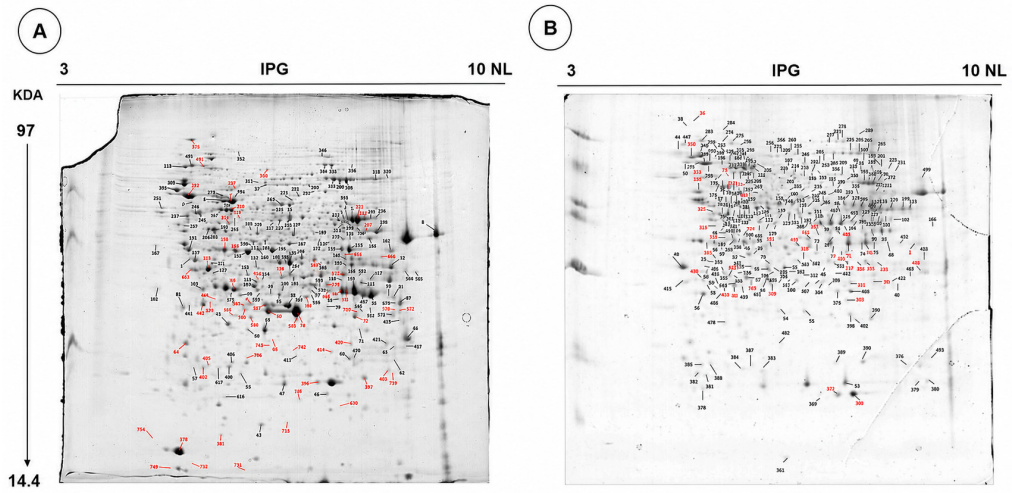

Figure 3. Reference map of the protein profile of the saprophytic mycelium of isolates Mp553 (**A**) and Mp565 (**B**) of the fungus *Moniliophthora perniciosa* under control conditions and treated with AWF of the cocoa genotypes TSH1188 and Catongo. The identification numbers in black represent the spots identified and that did not present differential accumulation between the treatments; those in red correspond to the spots that presented differential accumulation ($p \leq 0.005$ and fold ≥ 1.5) between the Crtl, Cat and TSH treatments. Representative gels for each treatment condition are shown in Supplementary Figure S2.

Comparative analysis of the reference maps revealed distinct patterns of differential spot modulation between the isolates in response to the AWF treatments. Mp553 showed a greater number of differentially accumulated spots in response to Cat AWF relative to its

control condition, whereas Mp565 presented more pronounced differential spot modulation in response to TSH AWF.

A total of 533 proteins were identified by LC-MS/MS from differential spots detected across all treatments, including 215 proteins from Mp553 and 318 proteins from Mp565 (Supplementary Table S1). An overview of the proteins identified from isolates Mp553 and Mp565, with significant or non-significant accumulation ($p \leq 0.005$; $p \geq 0.005$) and differential accumulation (LogFC ≥ 1.5), are represented in Figures 4 and 5 by red dots (identified, induced and significant proteins); blue dots (identified, suppressed and significant proteins) and gray dots (identified and non-significant proteins).

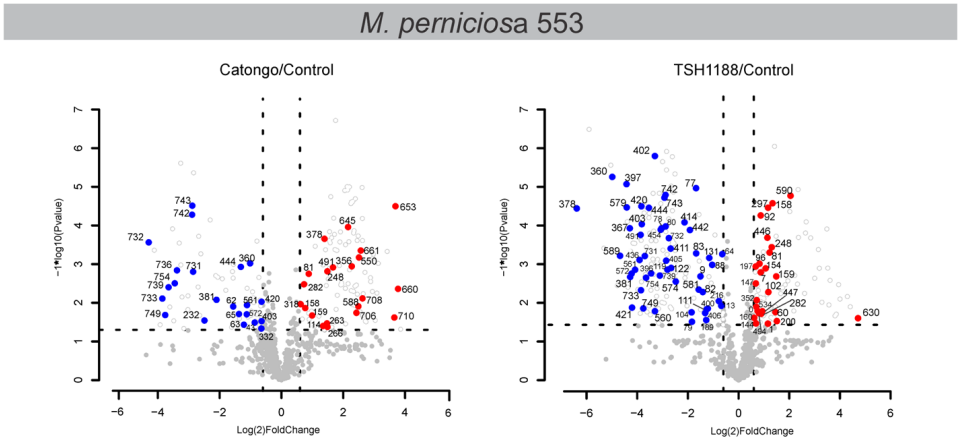

Figure 4. Variation in the differential accumulation of proteins identified in the *Moniliophthora perniciosa* isolate Mp553 for the treatments with AWF, Catongo (Cat) and TSH11888 (TSH) compared to the control condition. Proteins with reduced accumulation are represented by blue dots and those with increased accumulation by red dots. Gray dots represent differential proteins, but not statistically significant. (*) multiplication mathematical operator.

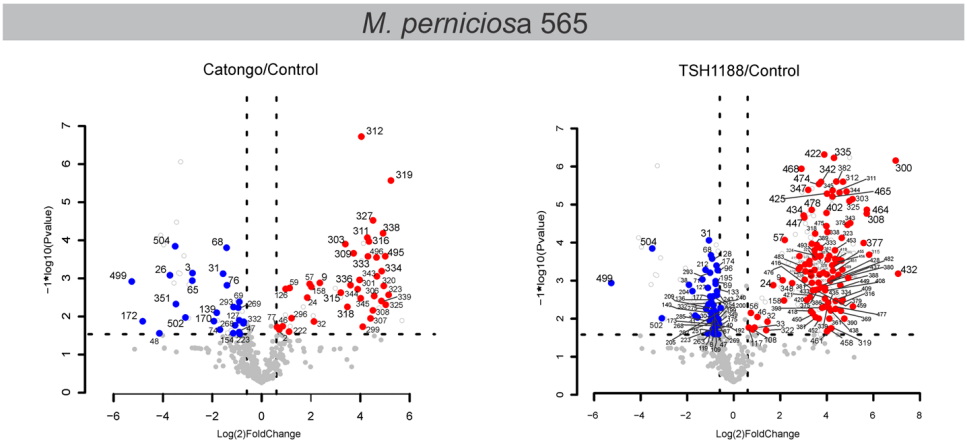

Figure 5. Variation in the differential accumulation of proteins identified in the Mp565 isolate for the treatments with AWF, Catongo (Cat) and TSH11888 (TSH) compared to the control condition (Ctrl). Proteins with reduced and increased accumulation are represented by blue and red dots, respectively. Gray dots denote differential proteins, but not statistically significant. (*) multiplication mathematical operator.

In the Mp553 isolate (Figure 4), considered less aggressive, of the 215 proteins identified, 143 were significant ($p \leq 0.005$). With regard to the accumulation profile of Mp553 proteins, those that presented reduced accumulation stood out in the AWF treatments of TSH and Cat.

The most aggressive isolate, Mp565, had more proteins with increased accumulation for the treatment of AWF of TSH, a more resistant cocoa variety, when compared to AWF of Cat (Figure 5). Mp565 grown in AWF of TSH contained 179 identified and significant proteins, a quantity twice as high as Mp553 in the same treatment (Supplementary Table S1). For the most aggressive isolate, there were a total of 246 identified and significant proteins.

2.3. Differential Protein Profile

The accumulation profiles of differentially accumulated proteins ($|\text{LogFC}| \geq 1.5$) are represented in Figure 6, and the corresponding protein identifications are listed in Supplementary Table S2. In total, 278 proteins were differentially accumulated in *M. perniciosa* in response to AWF from the cacao genotypes TSH1188 and Catongo relative to the control condition without AWF (Ctrl). Among these proteins, 181 in isolate Mp565 (Figure 6A) and 97 were also identified in isolate Mp553 (Figure 6B). Hierarchical cluster analysis grouped the differentially accumulated proteins according to similarities in their accumulation profiles across treatments, resulting in four major clusters for each isolate (Figure 6). Although some clusters showed gradual transitions in accumulation patterns, distinct treatment-associated modulation trends were observed between the isolates.

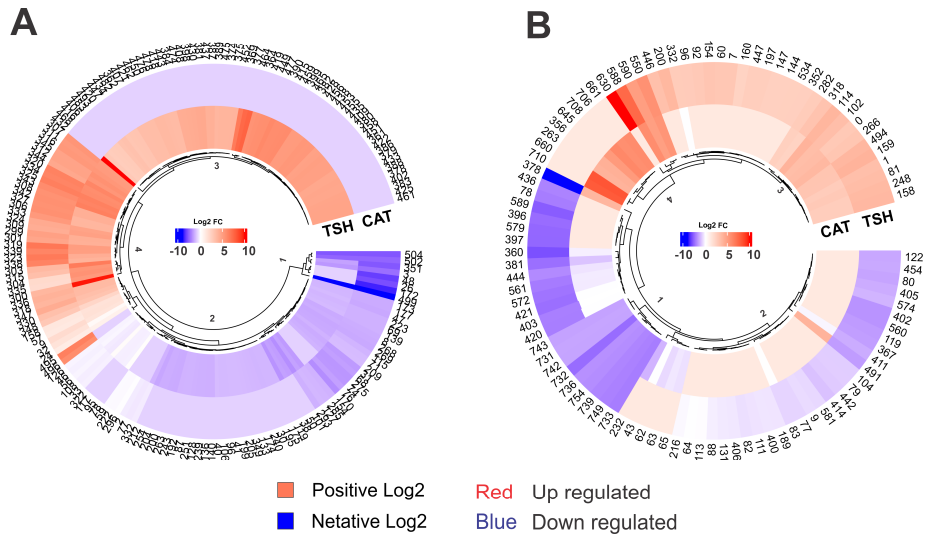

Figure 6. Heatmap with Euclidean distance representing identified and differentially accumulated proteins of isolates Mp565 (**A**) and Mp553 (**B**) of the fungus *Moniliophthora perniciosa* treated with AWF from cocoa varieties Catongo (Cat) and TSH1188 (TSH) compared to the control condition (without addition of AWF). In red, proteins with increased accumulation; in blue, proteins with reduced accumulation.

In Mp565 (Figure 6A), cluster 3 showed a dynamic accumulation profile in response to the AWF treatments. Proteins in this cluster were predominantly up-accumulated in the presence of TSH AWF and down-accumulated under Cat AWF treatment. This cluster included hypothetical proteins (IDs 369, 377, 425, 443 and 477) as well as proteins associated with cellular energy metabolism (Supplementary Table S2). In cluster 4, proteins were predominantly up-accumulated under both Cat and TSH AWF treatments. These proteins were mainly associated with oxidation-reduction processes, acetate metabolism, and carbon metabolism.

In Mp553 (Figure 6B), cluster 1 was predominantly composed of proteins down-accumulated in response to both AWF treatments. Cluster 2 contained mostly down-accumulated proteins or proteins with LogFC values close to zero, although it included an aldo-keto reductase protein (ID 491) showing the highest positive LogFC value within this group. Cluster 4 comprised proteins with greater accumulation under Cat AWF

treatment, including proteins related to cellular respiration, energy production, stress-response regulation, and redox signaling (IDs 660, 710, 708, 661, 706, 645, 356 and 263; Supplementary Table S2).

2.4. Functional Classification of Proteins

We used the Gene Ontology (GO) database for functional classification of only the identified and differentially significant proteins ($p \leq 0.005$ and fold ≥ 1.5). The number of proteins of the *M. perniciosa* isolates varied in response to Cat AWF and TSH in both isolates, and the number of proteins modulated in response to TSH AWF was higher than those induced by Cat AWF. This finding may be associated with the resistance of the genotype and mainly the number of exclusive spots observed in response to this treatment (Supplementary Tables S1 and S2).

Figure 7 represents the functional categorization of proteins from the Mp553 isolate subjected to AWF of Cat and TSH.

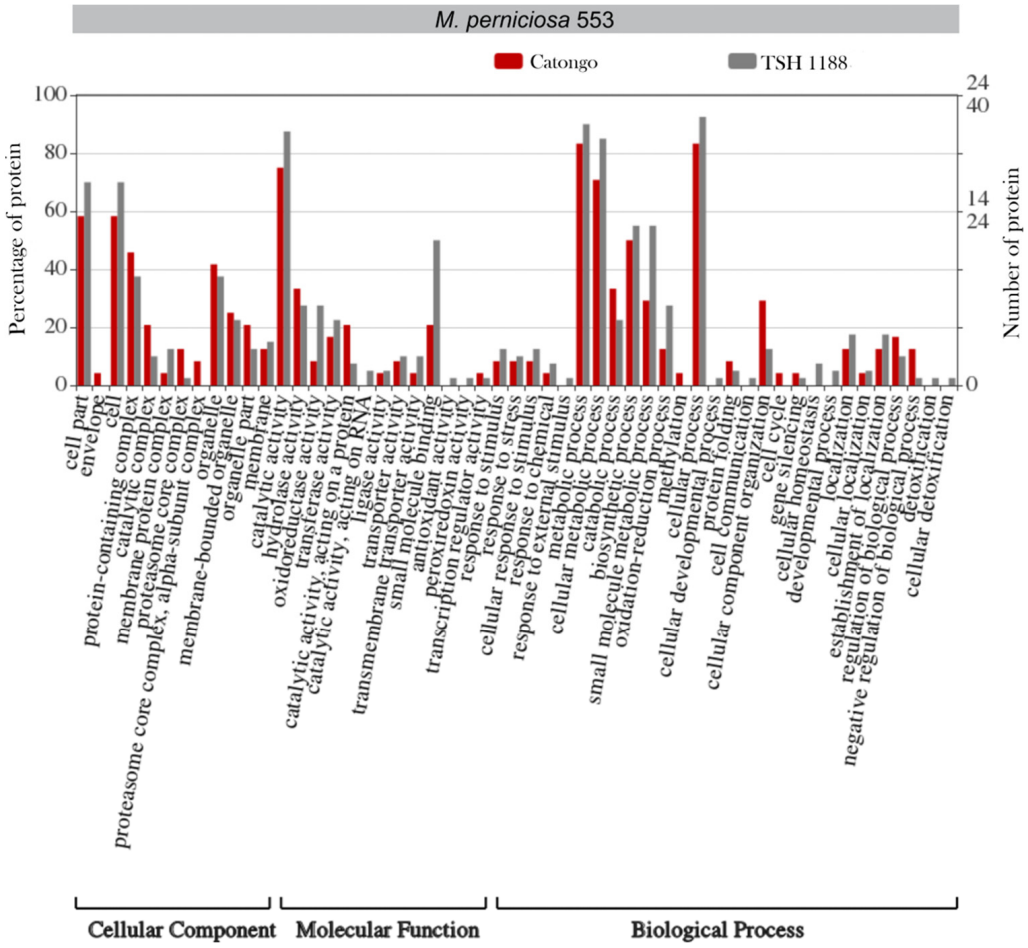

Figure 7. Functional categorization of proteins differentially expressed in the mycelium of *Moniliophthora perniciosa* isolate Mp553, treated with AWF from the cocoa varieties Catongo (Cat) and TSH1188 (TSH), compared to the control condition (Ctrl). The vertical axes represent the percentage and quantity of proteins found in the enriched functional category. Protein functions were categorized according to the cellular component (CC), molecular function (MF) and biological processes (BP), represented on the horizontal axis of the Figure.

The Biological Processes (BP) category was the most represented among the proteins identified in Mp553. Most of these were related to the fungal metabolism, acting in metabolic, catabolic, biosynthetic and cellular processes, totaling 70–90% of the proteins

when subjected to AWF of *T. cacao* genotypes. Still regarding BP, proteins related to detoxification, peroxidation and antioxidation were detected in the Mp553 isolate only in the treatment with AWF of TSH.

In the Molecular Function (MF) and Cellular Component (CC) categories, proteins with stress response function, as well as catalytic, hydrolase and oxidoreductase activities, showed between 45 and 85% accumulation in their respective functions for the Mp553 isolate in both AWF treatments.

The functional categories of proteins from isolate Mp565 when elicited by AWF of Cat and TSH are depicted in Figure 8.

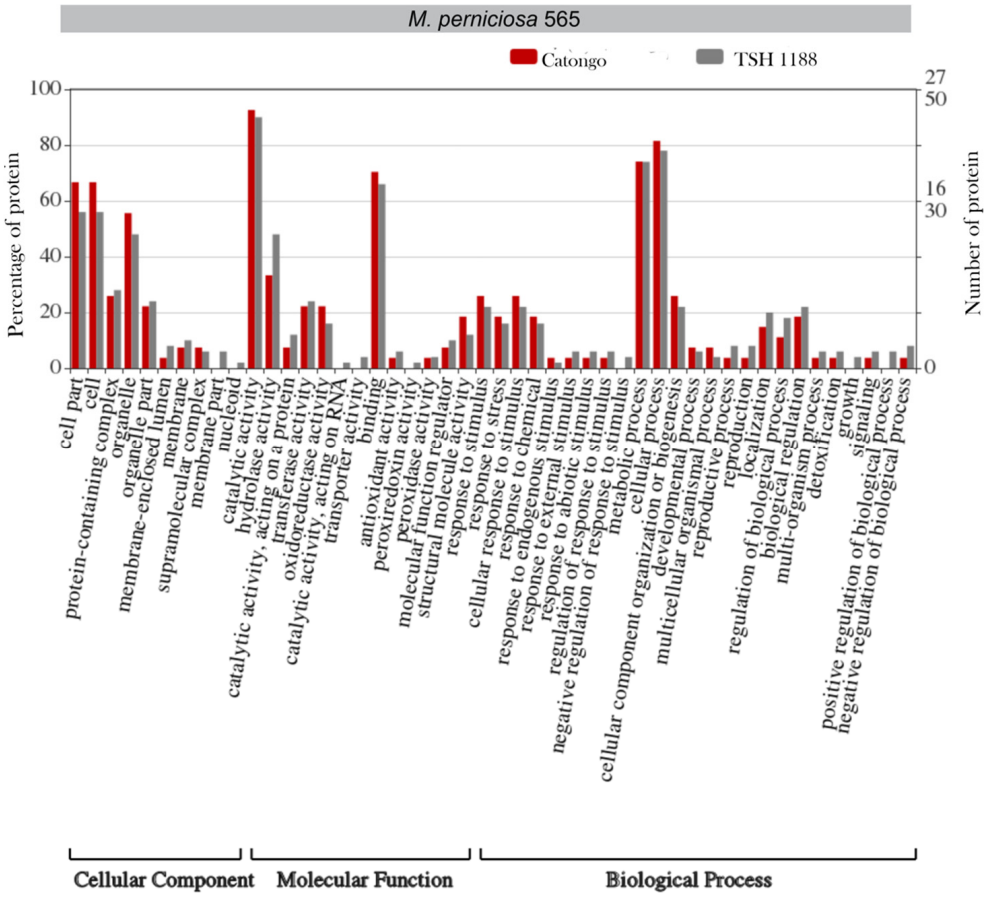

Figure 8. Functional categorization of proteins differentially expressed in the Mp565 isolate elicited by AWF from the cocoa varieties Catongo (Cat) and TSH1188 (TSH) compared to the control condition (Ctrl). The vertical axes represent the percentage and quantity of proteins found in the enriched functional category. Protein functions were categorized according to the cellular component (CC), molecular function (MF) and biological processes (BP), represented on the horizontal axis of the Figure.

The largest set of proteins was functionally associated with fungal metabolic processes, which were well represented for both AWF treatments, grouping 65–90% of the proteins. For isolate Mp565, few protein functions were present in only one of the treatments. Proteins related to nucleotides (2%), transport activity (5%), and pexoreduction (3%), even at low levels, were only present when isolate Mp565 was elicited with AWF from TSH—the most resistant cocoa variety.

In the BP category, proteins related to stimulus response, stress response, detoxification, localization, and signaling were induced by Mp565 under both AWF treatments. Proteins related to antioxidant activities, peroxidase activities, and binding were well represented in

MF. Likewise, proteins related to hydrolase and catalytic activities were well represented in the CC category.

2.5. Protein–Protein Interaction

The physical or functional interactions between the studied proteins are represented graphically and mathematically in the protein–protein interaction network (PPI) in Figures 9 and 10.

The protein network of the Mp553 isolate (Figure 9) contains 1182 nodes (proteins), 18,057 connectors and 17 clusters. Two hundred and thirteen proteins in the network are bottlenecks and 440 are hubs.

Cluster 2 has the largest number of nodes (proteins) in comparison with the others. These proteins are functionally associated with nitrogen compound metabolism. Also in this cluster, the protein with the highest betweenness and node degree value in the network was present, MPER_11800, showing an up-accumulated expression profile in the TSH AWF and down-accumulated in the Cat AWF. Proteins with high average betweenness and node degree values are considered important regulators of the PPI network.

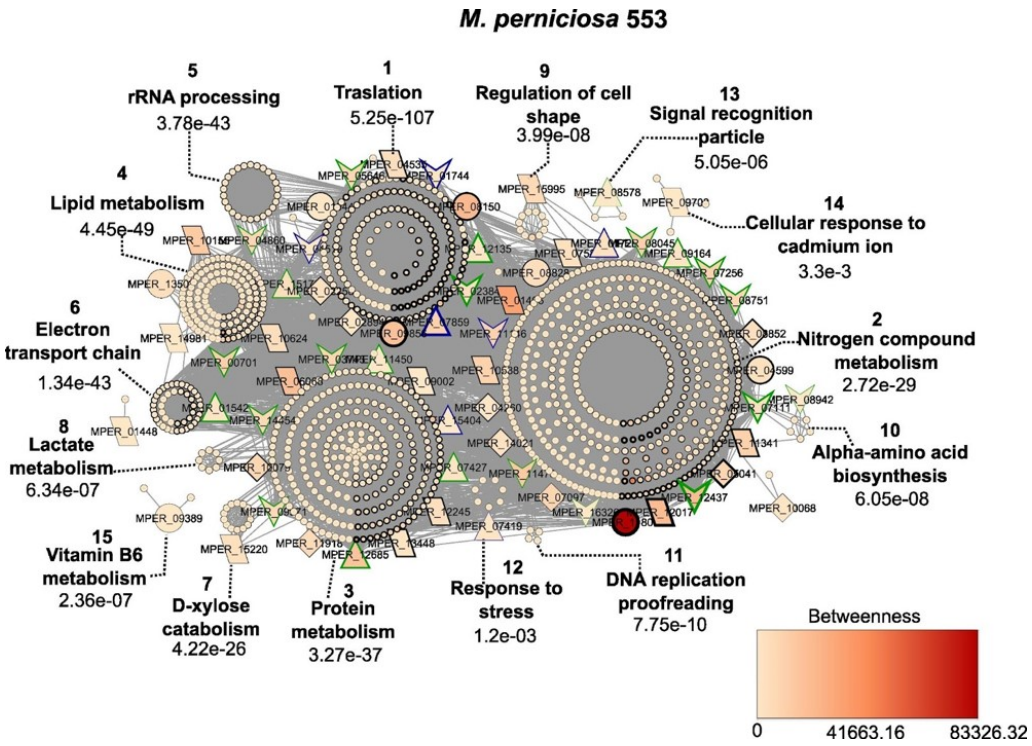

Figure 9. Differentially expressed Mp553 proteins subjected to PPI analysis. Each node represents a protein. Larger nodes represent the identified differentially expressed proteins. Larger triangle-shaped nodes represent proteins that had increased accumulation only in TSH1188 (green border) or only in Catongo (blue border). Nodes in the shape of an inverted triangle represent proteins with decreased accumulation only in TSH1188 (green border) or only in Catongo (blue border). Diamond-shaped nodes represent proteins that had increased accumulation in both TS118 and Catongo. Parallelogram-shaped nodes represent proteins that had decreased accumulation in both TSH1188 and Catongo. Larger circle-shaped nodes represent proteins with other accumulation pattern combinations. The border width is proportional to the node degree value. The betweenness value is represented by the fill color of each node. Each grouping of nodes represents a cluster. For each cluster, a biological process was assigned, according to the functional enrichment analysis performed in String, with the value of the false discovery rate (FDR).

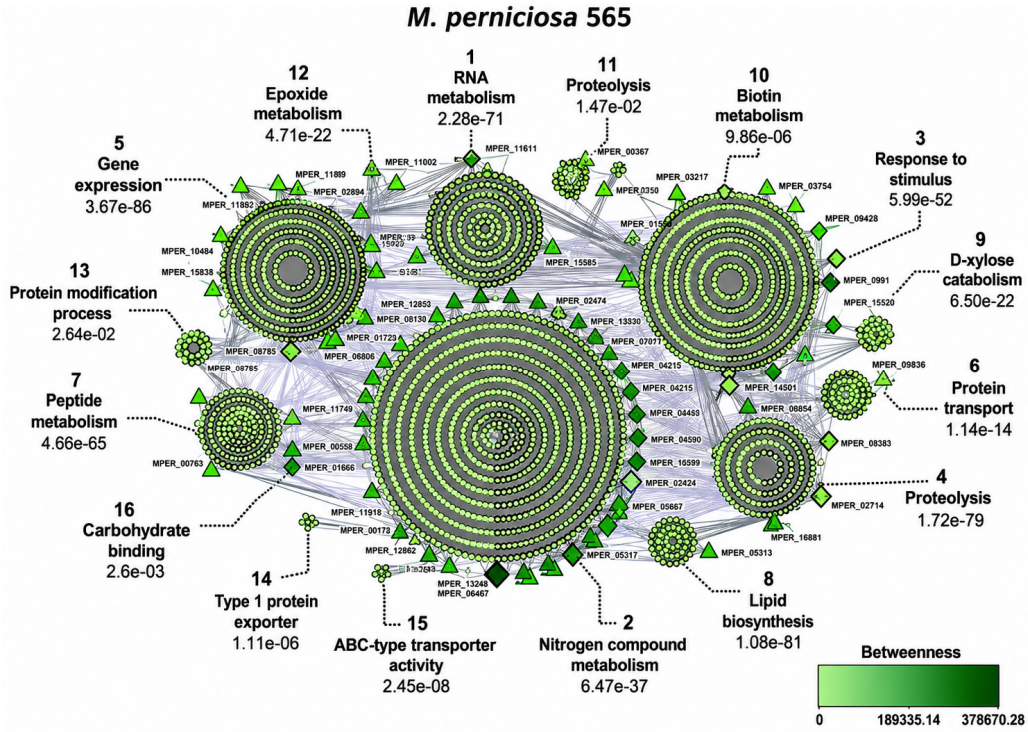

Figure 10. Differentially expressed proteins of Mp565 submitted to PPI analysis. Each node represents a protein. Larger nodes represent the identified differentially expressed proteins. Larger triangle-shaped nodes represent proteins that had increased accumulation only in TSH1188 (green border) or only in Catongo (blue border). Inverted triangle-shaped nodes represent proteins with decreased accumulation only in TSH1188 (green border) or only in Catongo (blue border). Diamond-shaped nodes represent proteins that had increased accumulation in both TS118 and Catongo. Parallelogram-shaped nodes represent proteins that had decreased accumulation in both TSH1188 and Catongo. Larger circle-shaped nodes represent proteins with other combinations of accumulation patterns. The width of the border is proportional to the node degree value. The betweenness value is represented by the filling color of each node. Each grouping of nodes represents a cluster. A biological process was assigned to each cluster, according to the functional enrichment analysis performed in String, with the false discovery rate (FDR) value.

Cluster 3 of the Mp553 isolate network group proteins was associated with fungal metabolism (3.27×10^{-37}) when in contact with AWF. In this cluster, proteins with increased accumulation only in TSH AWF (triangle with green border) and with exclusive increase in Cat AWF (triangle with blue border, one protein) were detected. None of the proteins associated with fungal metabolism showed decreased accumulation in the Cat AWF treatment (inverted triangle with blue border). However, *M. perniciosa* showed different metabolism when in contact with TSH AWF, reducing the accumulation of some proteins (inverted triangle with green border).

Cluster 12 associated with stress response is represented by a protein that shows increased accumulation in Mp553 when elicited with Cat AWF (blue-bordered triangle). Other proteins identified in Mp553 act in biological processes associated with translation (5.25×10^{-107}), regulation of cell shape (3.99×10^{-8}) and lipid metabolism (4.45×10^{-49}), among others (Figure 9).

The protein interactions of the Mp565 isolate are graphically represented in Figure 10. The PPI network of Mp565 is composed of 2771 nodes (proteins), 56,445 connectors and 17 clusters. Four hundred and thirty-nine proteins in this network are bottlenecks and 1048 have hub profiles.

The biological processes stand out, evidencing the efficiency of the fungus in circumventing the plant defense mechanism, represented by the AWF of Cat and TSH. Proteins

related to the response to stimulus (5.99×10^{-52}) were grouped in cluster 3. These proteins showed increased accumulation only in the AWF of TSH (triangle with green border), while others showed increased accumulation in both AWF treatments (diamond). On the other hand, proteins such as MPER_09428 showed decreased accumulation in both the AWF of TSH1188 and Catongo (parallelogram).

Biological processes, such as protein transport (1.14×10^{-14}), proteolysis (1.72×10^{-79}) and gene expression (3.67×10^{-86}), are well represented in the Mp565 PPI network. Cluster 2, which contains proteins associated with the metabolism of nitrogen compounds (6.47×10^{-37}), has the largest number of nodes. It contains the protein with the highest betweenness and node degree in the network, MPER_11800, which has increased accumulation when elicited with AWF of TSH and Cat (Figure 10).

3. Discussion

Proteomic and molecular studies of witches' broom mostly focus on the pathogen or the plant [21–26], which reinforces the need to investigate events that occur during the specific interaction between *T. cacao* and *M. perniciosa*, especially proteomic studies. Few studies have examined the apoplastic space as a scenario for responses in this interaction, and when carried out, they focused on the apoplastic proteomic mapping of *T. cacao* contrasting for resistance to WBD in the early phase of the disease [16,17]. In this study, aiming to understand the role of the apoplast in the interaction, we shed light on the dikaryotic mycelial protein profile of contrasting *M. perniciosa* isolates regarding pathogenicity, elicited with AWF from *T. cacao* genotypes that differ in their response to infection.

The protein composition of the apoplast and its importance were demonstrated in studies with potato tubers in response to stress, which identified twice as many hydrophobic proteins in the apoplast of healthy resistant potato tubers compared with susceptible ones [27]. The protein composition of the apoplastome of *T. cacao* was also revealed, indicating the presence of defense proteins in the apoplastic space of the plant when infected by *M. perniciosa* [17]. However, to date, the apoplast has been explored mainly from the perspective of the host plant, rather than the pathogen. Thus, this study, by investigating the proteomic response of the dikaryotic mycelium of *M. perniciosa* to the apoplastic fluid of *T. cacao*, mimicking the extracellular environment in which the fungus establishes itself during infection, provides an innovative approach that allows a deeper understanding of fungal adaptation to apoplast conditions and the possible mechanisms involved in fungal pathogenicity.

Here, apoplastic proteomic mapping of *M. perniciosa* isolates elicited by AWF of *T. cacao* genotypes resulted in a total of 1272 proteins detected in the protein profiles of Mp553 (755 proteins) and Mp565 (517 proteins). The analysis of the total number of spots obtained for the protein profiles of the isolates (Figure 3) suggests a specific response of *M. perniciosa* related to the cocoa varieties under study, since a significant number of exclusive spots (89) were observed for AWF of Cat in the Mp553 profile, and 138 exclusive spots of Mp565, in response to AWF of TSH.

The difference observed in the number of proteins modulated in Mp565 may also be due to the fact that we identified 103 more proteins in Mp565 (318 proteins identified) compared to Mp553 (215 proteins identified) (Figure 5 and Supplementary Table S1). Studies of molecular mechanisms in cocoa clones have revealed that an inducer-response mechanism is induced in tolerant cocoa clones [28]. This suggests early detection of the pathogen by the plant and induction of the defense response, which may explain the greater number of proteins identified in the Mp565 isolate, which is considered more aggressive when elicited in the AWF of susceptible and resistant cocoa plants.

3.1. Modulation of Proteins with Metabolic Functions and Biosynthetic Processes

Differentially expressed proteins showed proportional expression in both isolates, since more proteins were identified from isolate Mp565 than from Mp553. As shown in Figure 6, most of them are up-accumulated in both *M. perniciosa* isolates. However, when observing the Cat and TSH treatments, the regulation of the proteins is contrasting between the conditions in the different isolates.

Aldo-keto reductase (spot 743), and cysteine peroxiredoxin (spot 396) proteins are down-accumulated when elicited with AWF from the resistant cocoa variety TSH to isolate Mp553 (Figure 6B and Supplementary Table S2). This widespread suppression of differentially expressed proteins in the isolate corroborates the resistance of the TSH variety in the presence of *M. perniciosa* infection [29–31].

The largest number of identified and differentially expressed proteins are related to metabolism, energy and biosynthetic processes (Figures 7 and 8—Supplementary Table S2).

Proteins such as phosphoglycerate kinase (PGK), fructose-bisphosphate aldolase, glyceraldehyde-3-phosphate dehydrogenase (GAPDH) and the enolase protein were identified as composing the glycolytic pathway of isolates Mp553 and Mp565, as well as triose phosphate isomerases, acetyl transferases, aspartate amino transferases, enolase and 14-3-3 are also important in different biosynthetic processes of *M. perniciosa* isolates (Supplementary Table S2). The induction of these proteins favors the maintenance of ATP production by the fungi. In addition, they can act as elicitors, since glycolytic enzymes of *Candida albicans* can elicit an immune response in humans [32–36].

The incorporation of some immunogenic cytosolic proteins, such as enolase and heat shock protein (HSP) in the fungal cell wall may be a virulence mechanism for fungal survival [37]. These proteins, designated multifunctional, such as fructose-bisphosphate aldolase, triose phosphateisomerase, glyceraldehyde-3-phosphate dehydrogenase and enolase, were identified in our analyses.

The PGK protein was detected with increased accumulation in both isolates Mp553 and Mp565, with Mp565 having greater accumulation in the treatment with Cat AWF. This protein, in addition to composing the glycolytic pathway, also has protein phosphorylation activity, since it is a cell wall protein as demonstrated in *C. albicans* [33,35].

Enolase was also identified in both *M. perniciosa* isolates and was positively accumulated (spot 154) in the AWF TSH treatment (Supplementary Table S2). Enolase is an important enzyme of glycolysis, also considered to be one of the main cell wall proteins associated with glucans. The fact they are associated with the wall may facilitate their translocation; therefore, they are immunogenic proteins [36,38,39].

GAPDH, traditionally known for its role in glycolysis, has also been described as a moonlighting protein involved in adhesion and interaction with host extracellular matrix components in various fungal pathogens [40,41]. In our analyses, we identified a significant number of this protein, with six spots for Mp553 and eight spots for Mp565. In the most aggressive isolate—Mp565—when treated with the AWF of the most resistant variety—TSH—the GAPDH (spot 449) was shown to be up-accumulated in this condition, which was not observed in the Cat treatment (Figure 6A).

The gene encoding of this protein was predicted and identified in the *M. perniciosa* × *T. cacao* pathosystem, which shows that this protein is essential in the interaction of the fungus. In other studies with *M. perniciosa* infecting the TSH1188 cocoa variety, GAPDH proteins were also identified, with attribution of their function not only in the glycolytic pathway of *M. perniciosa*, but also in the transduction of ROS signaling [26,42]. Its modulation under AWF exposure suggests it may contribute not only to energy metabolism but also to fungal adaptation and host colonization.

Acetyl-CoA CoA C-acetyltransferase proteins, also called 2-methylacetoacetyl thiolase and acetyl-CoA hydrolase, were identified in isolates Mp553 and Mp565 in response to AWF treatments, and were modulated according to the cocoa varieties. They were always induced when the isolates were elicited by the TSH AWF in Mp565 (Supplementary Table S2), which suggests a mechanism to maintain membrane integrity and protein acetylation as a response of the fungus to the plant defense constituents present in the AWF. The reason for this is that these proteins may be involved in the biosynthesis of ergosterol, a specific lipid of fungi essential for the cell wall. Its absence can cause changes in membrane permeability and growth inhibition. For these reasons, the ergosterol biosynthesis pathway is an important target for the development of antifungal drugs [43,44].

Although our study focused on the proteomic modulation of *M. perniciosa*, the observed changes in protein accumulation suggest that AWF may exert physiological effects on fungal isolates. Notably, the modulation of proteins involved in oxidative stress response, energy metabolism (e.g., PGK, GAPDH, enolase), and protein folding (e.g., heat shock proteins) in both isolates—especially in Mp565 treated with AWF from the resistant genotype—indicates a possible adjustment of cellular processes in response to the apoplastic environment.

While direct physiological parameters such as hyphal growth, morphology, or sporulation were not assessed in this study, the proteomic shifts imply that AWF may influence fungal physiology at multiple levels. This highlights the importance of further studies integrating proteomics with phenotypic and physiological analyses to better understand fungal adaptation to host-derived signals.

3.2. Alteration in Protein Synthesis and Folding of Isolates Leads to Protein Reprogramming

The modulation of proteasomal proteins was observed specifically in isolates Mp553 and Mp565 in response to AWF treatments, together with the induction of other eukaryotic factors, indicating the occurrence of protein reprogramming of *M. perniciosa* in response to the *T. cacao* genotypes (Supplementary Table S2). The proteasome is essential for the dynamic regulation between the synthesis and degradation of proteins, such as those with folding errors, in addition to degrading proteins covalently linked by ubiquitins. This proteolytic activity is ATP-dependent [45].

We identified numerous "heat shock" proteins (HSP). The positive induction of these proteins is evidenced in Mp553 in response to Cat and TSH AWF, while in Mp565 they have a dynamic profile for both treatments (Supplementary Table S2). HSPs work to maintain proteins in their correct conformation (folding) and prevent protein aggregation in organisms subjected to stress, as well as in normal cellular processes [46,47]. Due to the importance of their functions, several studies have shown that these proteins have greater expression in response to various abiotic and biotic stresses [45]. The hostile plant environment in response to infection can cause protein unfolding and increased expression of fungal HSPs, suggesting greater resistance of *M. perniciosa* to the plant stress environment during infection [48].

The specific increase in HSP observed in Mp553 in response to TSH AWF treatment (Supplementary Table S2) suggests that constituents of the AWF from resistant cocoa varieties may signal protective proteins of the fungus *M. perniciosa*.

3.3. Upregulation of Signal Cascades Among Isolates Elicited by Cocoa AWF

Some proteins were identified with functions related to signal transduction, such as 14-3-3; ATPases, Ran-specific GTPase activating protein, and GTP-binding protein (Supplementary Table S2). In a broader analysis, proteins with functions related to signal transduction were modulated in both isolates Mp565 and Mp553.

GTPase proteins are a large family of hydrolase enzymes (GTP hydrolysers) with RanA domain, known to be up-accumulated in the early phases of yeast growth. These proteins are involved in facilitating the transport of compounds across the nuclear membrane, as well as in the regulation of mitotic activity [49]. In our analyses, Ran-specific GTPase activating proteins were downregulated in the Mp553 isolate by AWF TSH treatment.

Cytochrome B5 was exclusive to isolate Mp553, but was suppressed in the AWF treatments of Cat and TSH (Supplementary Table S2). The P450 family, which contains cytochrome B5 proteins, is extensive in basidiomycete fungi and plays an important role in the secondary metabolism of these fungi. Functional analysis and gene expression profiling data suggest that members of the P450 families are catalytically versatile and are possibly involved in fungal colonization of plant material [50,51].

Proteins from signaling pathways have been shown to be crucial for the virulence of several phytopathogenic fungi [52].

3.4. Differential Modulation of Defense Proteins and Oxidation Reduction

Biological processes involving defense and redox proteins were significantly enriched in both *M. perniciosa* isolates when elicited in AWF of the cocoa varieties TSH1188 and Catongo (Figures 7 and 8).

Proteins such as Erylysin B, 14-3-3, cyclophilins and HSPs are also involved in defense response (Supplementary Table S2).

14-3-3 is a protein that plays a role in the development and response to stress, since it acts in several biological processes through protein–protein interactions. For instance, it can modulate the expression of stress-inducible genes by regulating the activity and/or localization of transcription factors, in addition to having an anti-apoptotic function [53–55]. The 14-3-3 protein was not identified in the Mp553 isolate, only in Mp565, exclusively in response to TSH AWF (Supplementary Table S2).

Cyclophilins were detected only in the treatment with AWF of TSH, in Mp565. According to Chen et al. [56], cyclophilins are necessary for the virulence of the phytopathogenic fungus *Cryphonectria parasitica*. Studies with *Saccharomyces cerevisiae* indicate that the overexpression of cyclophilin A promotes tolerance to several stresses such as oxidative stress by metals and hydrogen peroxide [57]. Therefore, cyclophilin A is one of the promising targets for the development of antifungal drugs, and its molecular structure has already been elucidated in *M. perniciosa* [58]. The fact that isolate Mp565 is more aggressive and causes disease in both varieties of *T. cacao* corroborates the observation of these proteins in our analyses and suggests the importance of the cyclophilin in the pathogenicity of *M. perniciosa*.

3.5. Hypothetical Proteins

Studies of the *M. perniciosa* and *T. cacao* pathosystem have been conducted, along with sequencing the cDNA of *M. perniciosa* at different stages of its life cycle [59], the transcriptome [60], the genome and effectorome sequencing of different isolates [61]. Still, there are many genes that are annotated as encoding hypothetical proteins, whose existence is predicted, but without experimental evidence that they are expressed in vivo. However, these hypothetical proteins may be key players in the infection process of *M. perniciosa* in *T. cacao* plants, so they need further investigation.

Our results identified proteins annotated as hypothetical for the two *M. perniciosa* isolates, Mp565, but with functions annotated for other organisms as well (Supplementary Tables S1 and S2). Mp565 showed upregulated expression for the MPER_00772 protein predicted for *M. perniciosa* (spots 300, 369 and 377) when elicited

with TSH AWF (Supplementary Table S2). In a study of saprophytic mycelia of different *M. perniciosa* biotypes, Pierre et al. [62] also identified the mentioned protein as hypothetical.

Other hypothetical proteins were differentially expressed in the Mp565 isolate in the AWF Cat and TSH treatments, such as: MPER_00763, MPER_04035, MPER_06640 and MPER_04035. These proteins were first identified in the *M. perniciosa* genome sequence by Mondego et al. [63]. The MPER_04035 protein has also been identified as hypothetical in other studies of the fungus *Agaricus bisporus*, which also belongs to the basidiomycete class [64].

In the Mp553 isolate, only one protein with unknown function was statistically differential between the AF treatments, MPER_10538, which was also identified in the study by Modengo et al. [63].

Future studies are needed to investigate these hypothetical proteins, especially MPER_00772 found in *M. perniciosa* and never before detected in the proteome of other basidiomycete fungi. These proteins may promote important responses in the *M. perniciosa* and *T. cacao* pathosystem, depending on their function. They are also possible candidates for effector proteins that can facilitate infection or induce defense response mechanisms.

Thus, considering the significant number of proteins annotated as hypothetical in our study, and the potential role that they may play in the *M. perniciosa* × *T. cacao* interaction, we highlight the importance of using computational tools to advance functional prediction. Computational platforms that predict a three-dimensional structure of proteins with high accuracy or that integrate data from functional domains and protein families can be used to infer possible biological functions based on structural similarity and domain conservation [65,66]. The combination of these approaches can assist in the formulation of more targeted experimental hypotheses, allowing the prioritization of candidate proteins for future practical studies, such as heterologous expression, site-directed mutagenesis or interaction tests with host components.

3.6. Global Analysis of Proteins Through PPI Networks

The proteins identified and grouped in the different clusters in the PPI networks of the isolates Mp553 and Mp565, whether up- or down-accumulated, revealed an overview of the main development process of witches' broom, from the dikaryotic mycelia, in the transition phase of the disease still in contact with the apoplast, mimicking the in vivo condition (Figures 9 and 10).

Protein interactions in PPI networks are related to functional modules and protein complexes, as described by Wang et al. [67] and Spirin and Mirny [68], respectively. Functional modules are groups of proteins in which interactions occur at different locations or times, such as signaling proteins and metabolic pathways. Protein complexes participate in the molecular machinery that occurs in the same location.

The centrality values indicated that MPER_11800 is among the most important proteins for network regulation. This protein is present in cluster 2 of the networks of isolates Mp553 and Mp565, in both cases associated with the metabolism of nitrogen compounds, essential for the synthesis of vital biomolecules, elimination of toxins and regulation of cellular metabolism. Furthermore, this process is related to obtaining energy through this pathway, and these mechanisms are key for the development of the fungus and the disease [9]. In the Mp553 isolate, we identified proteins involved in cellular metabolism, a fact corroborated by the presence of 13 orthologous proteins in cluster 3, the third largest in the PPI network (Figure 9). Proteins involved in cellular metabolism are typically found in *M. perniciosa* during the early phase of infection [23,24].

The infection mechanisms of the Mp565 isolate, when elicited by AWF from *T. cacao* varieties, are illustrated in Figure 10, showing different protein components interacting

in several biological functions, such as response to stimuli, cellular metabolism, gene expression and proteolysis. These clusters do not represent isolated entities, but rather form a biological network of proteins in response to AWF, allowing us to infer the functional interactions of these macromolecules.

The second largest cluster in the PPI network of isolate Mp565, cluster 2, is associated with response to stimuli, with most orthologous proteins showing up-accumulation. This cluster significantly reflects the *M. perniciosa* × *T. cacao* interaction, since studies of the apoplastome of *T. cacao* genotypes have identified proteins related to defense and stress, with emphasis on pathogenesis proteins (PR proteins) [17]. Although PR proteins were not directly identified in the fungal proteome analyzed in the studied AWF, fungal proteins associated with defense processes and response to oxidative stress were significantly modulated in response to exposure to the apoplast (AWF) of *T. cacao*. Among them, catalase, oxidases, oxidoreductase, HSP, cyclophilin, and glutathione stand out (Supplementary Tables S1 and S2), with functions described in detoxification mechanisms, redox homeostasis, and stress tolerance. These proteins represent an adaptive response of *M. perniciosa* to the hostile apoplast environment, rich in antimicrobial compounds produced by the plant. The presence and induction of these proteins, conferred by cluster enrichment, reinforce the importance of the apoplast as a key microenvironment in plant–pathogen interactions, and highlight the potential of AWF components as elicitors of fungal proteomic reprogramming.

These interactions reveal that the proteins involved in the interaction between *M. perniciosa* and *T. cacao*, more precisely the fungus in contact with the apoplast, do not act in isolation. This sheds light on how these mechanisms are connected, making it possible to predict and understand new functional interactions in this pathosystem, corroborating the findings of Santos et al. [26], who also identified protein interactions in PPI networks involving the meristem of resistant cocoa plants infected by *M. perniciosa*.

Thus, the analysis of integrated PPI networks integrates and expands the findings obtained through differential proteomic analysis and functional categorization, reinforcing the biological relevance of proteins previously identified as differentially accumulated. For example, the protein MPER_11800, which presented high centrality in both networks (Mp553 and Mp565), was also identified among the differentially accumulated spots and is associated with the metabolism of nitrogen compounds—an essential pathway for fungal growth and adaptation to the apoplastic environment. Furthermore, the presence of clusters strongly connected to the response to stimuli, oxidative stress, and energy metabolism complements the functional data derived from the GO annotation, which indicated the induction of defense and metabolism proteins in response to the AWF of TSH1188. This convergence between the different levels of analysis—protein accumulation, functional categorization and network connectivity—strengthens the interpretation that AWF of contrasting *T. cacao* genotypes modulates not only the abundance but also the connectivity and functional importance of fungal proteins involved in adaptation and potential virulence. Thus, PPI networks provide a systemic view of the molecular interactions that underlie the adaptive response of *M. perniciosa*.

4. Materials and Methods

4.1. Biological Material and Cultivation of Moniliophthora perniciosa

The isolates FA553 (hereafter Mp553) and Mp565 used in this study were obtained from the João Louis M. Pereira Collection of *Moniliophthora* spp. maintained by CEPLAC/CEPEC in Bahia, Brazil, at the Plant Pathology Molecular Laboratory. These isolates are considered reference strains for *M. perniciosa* research. Mp553 has been widely used in genomic and

proteomic studies (e.g., Mondego et al. [63]), while Mp565 has also been utilized in studies assessing pathogen aggressiveness (Gramacho et al. [69], Santos et al. [70]).

Both isolates were previously characterized for their pathogenicity on *Theobroma cacao* by CEPLAC/CEPEC. Mp553 is less aggressive, whereas Mp565 is aggressive on TSH's clones (Jucá). It is worth mentioning that the *Theobroma cacao* genotypes used in this study present contrasts regarding resistance to witches' broom: TSH 1188 is considered resistant, while Catongo is highly susceptible to *M. perniciosa* [71,72].

The maintenance and cultivation of the isolates were carried out in solid mineral medium (glucose 1% (*w*/*v*), $NH_4H_2PO_4$ 0.1% (*w*/*v*), KCl 0.02% (*w*/*v*), $MgSO_4.7H_2O$ 0.02% (*w*/*v*), $CuSO_4$ 0.01% (*w*/*v*), $ZnSO_4.7\ H_2O$ 0.01% (*w*/*v*), yeast extract 0.5% (*w*/*v*), Agar 1.5% (*w*/*v*)) along with liquid extract, used for the experiments with AWF. The mycelia were grown in the dark at 25 °C in BOD for a period of 14 to 20 days.

4.2. Extraction of Apoplastic Washing Fluid from Theobroma cacao Leaves

To minimize physiological variability among plants and obtain representative apoplastic samples for each cocoa genotype, apoplastic fluid (AWF) was extracted from a set of mature leaves from three clonal plants of Catongo and TSH1188 under field conditions (with the presence of dry broomweed). The leaves were washed with distilled water and the midrib was removed and, then placed in a container with potassium phosphate at pH 5.5 and centrifuged at 4000× *g* at 4 °C, as described by Pirovani et al. [73]. They were used for AWF extraction by the VIC method.

AWF aliquots with a final volume of 15 mL from each cocoa genotype were obtained from a yield of ~240 µL g^{-1} of leaf. After extraction, the AWF samples were filtered through 0.22 µm membranes to remove cellular debris and potential microbial contaminants before lyophilization. The extracted AWF was lyophilized in a Freezone 6 freeze dryer (Labconco Corporation, Kansas City, MI, USA) for 48 h. Since the objective of this study was to evaluate fungal proteomic remodeling caused by apoplastic components of cocoa, protein identification, analyses were performed using the *M. perniciosa* database, and protein extracts were found exclusively from fungal mycelia washed after exposure to treatments with apoplastic fluid.

4.3. Cultivation of Moniliophthora perniciosa in Apoplastic Washing Fluid

Six dikaryotic mycelial disks of *M. perniciosa* isolates Mp553 and Mp565 were inoculated into independent Erlenmeyer flasks containing 30 mL of liquid mineral medium supplemented with streptomycin (10 mg mL^{-1}), chloramphenicol (34 mg mL^{-1}), and ampicillin (50 mg mL^{-1}). Two independent flasks were prepared for each treatment condition, representing biological replicates for each isolate and treatment combination. The flasks were incubated at 25 °C under gentle agitation for 7 days. Subsequently, the liquid medium was discarded and the mycelia were washed with sterile distilled water.

The dikaryotic mycelia were then transferred to fresh liquid mineral medium supplemented with the solid fraction obtained from 15 mL of lyophilized AWF from the Cat and TSH cacao genotypes, in addition to a control treatment without AWF supplementation. Samples of the three treatment conditions were incubated for 12 h at 25 °C. After incubation, the mycelia were washed, separated from the culture medium by filtration, frozen in liquid nitrogen, lyophilized, and stored at −80 °C until protein extraction.

For AWF preparation, mature leaves from five clonal plants of each cacao genotype were pooled prior to extraction in order to minimize plant-to-plant physiological variation and obtain representative apoplastic samples for each genotype.

4.4. Protein Extraction

Protein extraction from the dikaryotic mycelia of isolates Mp553 and Mp565 in AWF was performed according to Pirovani et al. [73].

Freeze-dried mycelial samples obtained from two independent biological replicates per treatment were ground in liquid nitrogen using a mortar and pestle until a fine powder (0.02–0.05 g) was obtained. Proteins were precipitated according to the protocol described by Pirovani et al. [73], and the resulting protein pellets were washed twice with cold 0.1 mol L^{-1} ammonium acetate in methanol, followed by two washes with cold 80% acetone. Supernatants were discarded after each washing step, and the protein pellets were dried at room temperature.

The samples were then solubilized in rehydration buffer containing urea (7 mol L^{-1}), thiourea (2 mol L^{-1}), CHAPS (1%), DTT (0.1 mol L^{-1}), IPG buffer (0.5%, pH 3–10 NL), and traces of bromophenol blue. Protein extracts obtained from mycelia exposed to AWF were quantified using the 2-D Quant Kit (GE Healthcare, Little Chalfont, UK), with bovine serum albumin (BSA; Sigma-Aldrich, St. Louis, MO, USA) used as standard.

4.5. 1D and 2D Two-Dimensional Electrophoresis

A 1D and 2D two-dimensional electrophoresis strategy was employed to enable the comparative visualization of proteomic remodeling induced the by cocoa AWF treatments, allowing the detection of differentially accumulated protein spots and potential isoform variations prior to LC-MS/MS identification.

The first dimension, consisting of isoelectric focusing (IEF), was performed by applying 350 µg of proteins from each sample in 13 cm strips, with an immobilized pH gradient from 3 to 10 NL. (pH 3–10 NL, 130 × 3 × 0.5 mm; GE Healthcare, Immobiline™ Dry-Strip). These strips were placed in an Ethan IPGphor III Isoelectric Focusing unit with the following steps: 1 h at 500 Vh; 1 h, 4 min at 1000 Vh; 2 h and 30 min at 8000 Vh. and 22 min at 8000 Vh at 20 °C. Then, the strips were treated (twice for 15 min) in equilibration buffer (urea 6 mol L^{-1}, SDS 2%, glycerol 30%, Tris–HCl 0.05 mol L^{-1}, pH 8.8) containing 1% DTT and 2.5% Iodoacetamide, in 1X running buffer (Tris, 0.025 mol L^{-1}, glycine 0.19 mol L^{-1}, SDS 0.1%, pH 8.3), under slow stirring.

The second dimension was carried out in polyacrylamide gel 12.5% (12 mL of 29.2%/and 0.8% (*w*/*v*) of acrylamide/bis-acrylamide, 7.5 mL of 1.5 mol L^{-1} Tris-HCl (pH 8.8), 0.15 mL of ammonium persulfate 10% (*p*/*v*), 0.02 mL of TEMED and 10.2 mL of water) in Hoefer SE 600 Ruby vertical electrophoresis system (Amersham Biosciences, Little Chalfont, UK). The equilibrated strips were placed on top of the gel and sealed with 1% agarose containing traces of bromophenol blue. A total of 3 runs of each sample were performed, with gel triplicates for each analysis.

The gels resulting from 2-DE electrophoresis were fixed in a solution containing 40% ethanol and 10% acetic acid for 1 h and finally transferred to Coomassie brilliant blue G-250 [74] for five days.

2-DE Image Analysis

The gel images were scanned with a LabScanner device (Amersham Bioscience) and analyzed with the ImageMaster 2D Platinum 7.0 (GE Healthcare) considering the area and intensity of the "spots", using normalization by total spot volume (total spot volume normalization), a standard method for correcting technical variations between gels. Control samples were compared with AWF-treated samples of the susceptible and resistant cocoa varieties, Catongo (Cat) and TSH1188 (TSH), respectively.

Statistical analysis was performed based on ANOVA between treatments (Ctrl × Cat, Ctrl × TSH, Cat × TSH), and the *p*-values obtained were adjusted using the Benjamini–

Hochberg FDR (False Discovery Rate) correction method. Spots with an adjusted p-value ≤ 0.005 and fold change ≥ 1.5 were considered differential.

4.6. Identification of Spots by Mass Spectrometry (LC/MS/MS)

Rather than aiming at exhaustive proteome coverage, the experimental design was focused on identifying major protein accumulation changes associated with fungal adaptation to contrasting cocoa apoplastic environments. Therefore, differential and exclusive spots were excised from the 2-DE gel and tryptic digestion was performed according to Shevchenko et al. [75]. Peptide mixtures were analyzed by online nano flow liquid chromatography tandem mass spectrometry (LC-MS/MS) with a nanoAcquity chromatograph (Waters, Milford, MA, USA) coupled to a Q-Tof micro mass spectrometer (Waters) [76].

4.7. Protein Identification

Raw MS and MS/MS data were processed by the ProteinLynx v2.3 software (Waters) and searched against the NCBInr database via the MASCOT server (http://www.matrixscience.com/, Accessed 5 January 2020). The parameters used for the searches were the following: digestion by the enzyme trypsin, carbamidomethyl (Cys) as fixed modification and oxidation (Met), as variable modification; maximum of one cleavage site loss; and ± 0.3 Da for the peptide tolerance error and 0.1 Da for fragment ion errors.

4.8. Annotation and Functional Categorization of Proteins

The FASTA sequences of the identified proteins were obtained from the accession numbers resulting from a search using the MASCOT software version 3.0 (http://www.matrixscience.com/). These sequences were subjected to functional annotation by the PANNZER2 software (http://ekhidna2.biocenter.helsinki.fi/sanspanz/, Accessed 26 June 2022) and subsequently categorized according to cellular functions and processes, namely: Biological Processes (BP), Molecular Function (MF) and Cellular Component (CC) with the WEGO software (version 2.0). The Pannzer2 and Wego tools were used to annotate and functionally categorize the identified and differentially significant proteins ($p \leq 0.005$ and fold ≥ 1.5). The Gene Ontology (GO) terms obtained from the Pannzer2 annotation were filtered based on PPV > 0.35, which corresponds to the positive predicted value that estimates the reliability of the predicted GOs for the annotated proteins. The proteins were categorized according to Molecular Function (MF), Biological Process (BP) and Cellular Component (CC).

4.9. Protein–Protein Interaction Network Analysis—PPI

PPI networks were formed considering differentially expressed proteins with fold value ≥ 1.5 and p-value < 0.005, using the String protein bank (version 12). The networks were constructed according to Mora-Ocampo et al. [77]. In the software, all analyses were performed against *M. perniciosa*, the standard organism. PPI information was obtained by enabling different prediction methods in the software, such as neighborhood, experiments, co-expression, gene fusion, databases and co-occurrence, in addition to the Cluster MCL clustering method. The functional enrichment analysis of the clusters was performed with the String tool.

5. Conclusions

Supplementation of culture medium with AWF from contrasting cacao genotypes induced significant proteomic remodeling in the dikaryotic mycelium of *M. perniciosa* isolates Mp553 and Mp565. Differential accumulation of proteins associated with glycolysis, protein synthesis, redox balance, and oxidative stress response suggests that exposure to cacao

apoplastic components triggers adaptive metabolic responses in the fungus, particularly in the more aggressive isolate Mp565.

The comparative proteomic profiles obtained in this study indicate that AWF from contrasting *T. cacao* genotypes differentially modulates fungal metabolism according to isolate aggressiveness, supporting the existence of a dynamic interaction at the apoplastic interface of the *M. perniciosa*–*T. cacao* pathosystem. The proteins identified here represent potential candidates associated with fungal adaptation and pathogenicity-related processes and may contribute to future functional investigations of the molecular mechanisms involved in witches' broom disease.

In addition, the use of cacao AWF as a culture medium supplement represents a promising experimental approach for investigating early molecular responses of *M. perniciosa* under conditions that partially simulate host interaction. This strategy may facilitate the identification of proteins potentially involved in fungal adaptation and host–pathogen communication during infection.

Supplementary Materials: The following supporting information can be downloaded at: https://www.mdpi.com/article/10.3390/stresses6020032/s1, Supplementary Figure S1; Supplementary Figure S2; Supplementary Table S1: Total spots identified—Mp553; Supplementary Table S2: Differentially expressed proteins identified—Mp553.

Author Contributions: L.R.C.: Experiment design, data curation, data analysis, investigation, methodology and writing—original draft. A.S.S.: Data curation, methodology, software and writing—original draft. I.Y.M.O.: PPI network data curation, software, methodology and writing—original draft. E.M.d.A.S.: Data curation, bioinformatics analysis and methodology. F.C.A.: Supervision and writing—original draft. K.P.G.: Methodology and supervision. C.P.P.: Conceptualization, funding acquisition, project administration, resources, supervision, and writing—original draft. All authors have read and agreed to the published version of the manuscript.

Funding: This work was supported by Coordenação de Aperfeiçoamento de Pessoal de Nível Superior—CAPES: 0001 and FAPESB/INCITE process number PIE0011/2026).

Institutional Review Board Statement: Not applicable.

Informed Consent Statement: Not applicable.

Data Availability Statement: All data generated or analyzed during this study are included in this article and its additional files.

Acknowledgments: We are grateful for the financial support provided by Coordenação de Aperfeiçoamento de Pessoal de Nível Superior (CAPES) and Fundação de Amparo à Pesquisa do Estado da Bahia (FAPESB).

Conflicts of Interest: The authors declare no competing interests.

Abbreviations

The following abbreviations are used in this manuscript:

AWF	Apoplastic washing fluid
WBD	Witches' broom disease
Ctrl	Control
Cat	Catongo
TSH	TSH1188
1D PAGE	One-dimensional electrophoresis
2D PAGE	Two-dimensional electrophoresis
LC-MS/MS	Liquid chromatography–mass spectrometry
PPI	Protein–protein interaction

References

1. Cocoa Processing Machinery Manufacturer. Available online: https://www.cocoamachinery.com/ (accessed on 15 April 2026).
2. ICCO International Cocoa Organization (ICCO). Available online: https://www.icco.org/ (accessed on 15 April 2026).
3. M'bo, A.A.K.; Cherif, M.; Kouadio, K.; Adolphe, M.G.; Bamba, A.; Toure, E.N.D.; Okou, A.K.; Brunelle, R.; Rouseau, Y.; Koné, D. Climate Variability and Outlook of Cocoa Production in Côte D'ivoire under Future Climate. In *Shifting Frontiers of Theobroma Cacao-Opportunities and Challenges for Production*; IntechOpen: London, UK, 2023. [CrossRef]
4. Katz, D.L.; Doughty, K.; Ali, A. Cocoa and chocolate in human health and disease. *Antioxid. Redox Signal.* **2011**, *15*, 2779–2811. [CrossRef] [PubMed]
5. Franco, R.; Oñatibia-Astibia, A.; Martínez-Pinilla, E. Health benefits of methylxanthines in cacao and chocolate. *Nutrients* **2013**, *5*, 4159–4173. [CrossRef]
6. Shahanas, E.; Panjikkaran, S.T.; Aneena, E.R.; Sharon, C.L.; Remya, P.R. Health benefits of bioactive compounds from cocoa (*Theobroma cacao*). *Agric. Rev.* **2019**, *40*, 143–149. [CrossRef]
7. Silva, S.D.V.M.; Matsuoka, K. Histologia da interaçao *Crinipellis perniciosa* em cacaueiros suscetível e resistente. *Fitopatol. Bras.* **1999**, *24*, 54–59.
8. Penman, D.; Britton, G.; Hardwick, K.; Collin, H.A.; Isaac, S. Chitin as a measure of biomass of *Crinipellis perniciosa*, causal agent of witches' broom disease of *Theobroma cacao*. *Mycol. Res.* **2000**, *104*, 671–675. [CrossRef]
9. Scarpari, L.M. Biochemical Changes during the Development of Witches' Broom: The Most Important Disease of Cocoa in Brazil Caused by *Crinipellis perniciosa*. *J. Exp. Bot.* **2005**, *56*, 865–877. [CrossRef]
10. de Oliveira Ceita, G.; Macêdo, J.N.A.; Santos, T.B.; Alemanno, L.; da Silva Gesteira, A.; Micheli, F.; Mariano, A.C.; Gramacho, K.P.; da Silva, D.C.; Meinhardt, L.; et al. Involvement of calcium oxalate degradation during programmed cell death in Theobroma cacao tissues triggered by the hemibiotrophic fungus *Moniliophthora perniciosa*. *Plant Sci.* **2007**, *173*, 106–117. [CrossRef]
11. Santos, A.S.; Mora-Ocampo, I.Y.; de Novais, D.P.S.; Aguiar, E.R.G.R.; Pirovani, C.P. State of the art of the molecular biology of the interaction between cocoa and witches' Broom disease: A systematic review. *Int. J. Mol. Sci.* **2023**, *24*, 5684. [CrossRef]
12. Farvardin, A.; González-Hernández, A.I.; Llorens, E.; García-Agustín, P.; Scalschi, L.; Vicedo, B. The apoplast: A key player in plant survival. *Antioxidants* **2020**, *9*, 604. [CrossRef]
13. Doehlemann, G.; Hemetsberger, C. Tansley review Apoplastic immunity and its suppression by filamentous plant pathogens. *New Phytol.* **2013**, *198*, 1001–1016. [CrossRef]
14. O'Leary, B.M.; Neale, H.C.; Geilfus, C.M.; Jackson, R.W.; Arnold, D.L.; Preston, G.M. Early changes in apoplast composition associated with defence and disease in interactions between Phaseolus vulgaris and the halo blight pathogen *Pseudomonas syringae* Pv. phaseolicola. *Plant Cell Environ.* **2016**, *39*, 2172–2184. [CrossRef] [PubMed]
15. Scalschi, L.; Llorens, E.; González-Hernández, A.I.; Valcárcel, M.; Gamir, J.; García-Agustín, P.; Vicedo, B.; Camañes, G. 1-methyltryptophan modifies apoplast content in tomato plants improving resistance against *Pseudomonas syringae*. *Front. Microbiol.* **2018**, *9*, 2056. [CrossRef]
16. de Oliveira, I.B.; Moura, I.M.; Santana, J.O.; Gramacho, K.P.; dos Santos Alves, S.; Ferreira, M.M.; Santos, A.S.; de Novais, D.P.S.; Pirovani, C.P. Cocoa apoplastome contains defense proteins against pathogens. *Phytopathology* **2024**, *114*, 427–440. [CrossRef] [PubMed]
17. de Oliveira, I.B.; Alves, S.D.S.; Ferreira, M.M.; Santos, A.S.; Farias, K.S.; Assis, E.T.C.D.M.; Mora-Ocampo, I.Y.; Muñoz, J.J.M.; Costa, E.A.; Gramacho, K.P.; et al. Apoplastomes of contrasting cacao genotypes to witches' broom disease reveals differential accumulation of PR proteins. *Front. Plant Sci.* **2024**, *15*, 1387153. [CrossRef]
18. Martínez-González, A.P.; Ardila, H.D.; Martínez-Peralta, S.T.; Melgarejo-Muñoz, L.M.; Castillejo-Sánchez, M.A.; Jorrín-Novo, J.V. What proteomic analysis of the apoplast tells us about plant–pathogen interactions. *Plant Pathol.* **2018**, *67*, 1647–1668. [CrossRef]
19. Wang, Y.; Wang, Y. Trick or treat: Microbial pathogens evolved apoplastic effectors modulating plant susceptibility to infection. *Mol. Plant Microbe Interact.* **2018**, *31*, 6–12. [CrossRef]
20. Hassett, K.; Ellwood, S.R.; Zulak, K.G.; Muria-Gonzalez, M.J. Analysis of apoplastic proteins expressed during net form net blotch of barley. *J. Plant Dis. Prot.* **2020**, *127*, 683–694. [CrossRef]
21. Gesteira, A.S.; Micheli, F.; Carels, N.; Da Silva, A.C.; Gramacho, K.P.; Schuster, I.; Macêdo, J.N.; Pereira, G.A.G.; Cascardo, J.C.M. Comparative Analysis of Expressed Genes from Cacao Meristems Infected by *Moniliophthora perniciosa*. *Ann. Bot.* **2007**, *100*, 129–140. [CrossRef]
22. Alvim, F.C.; Mattos, E.M.; Pirovani, C.P.; Gramacho, K.; Pungartnik, C.; Brendel, M.; Cascardo, J.C.M.; Vincentz, M. Carbon Source-Induced Changes in the Physiology of the Cacao Pathogen *Moniliophthora perniciosa* (Basidiomycetes) Affect Mycelial Morphology and Secretion of Necrosis-Inducing Proteins. *Genet. Mol. Res.* **2009**, *8*, 1035–1050. [CrossRef]
23. Mares, J.H.; Gramacho, K.P.; Dos Santos, E.C.; Santiago, A.D.S.; Silva, E.M.D.A.; Alvim, F.C.; Pirovani, C.P. Protein Profile and Protein Interaction Network of *Moniliophthora perniciosa* Basidiospores. *BMC Microbiol.* **2016**, *16*, 120. [CrossRef]

24. Mares, J.H.; Gramacho, K.P.; Santos, E.C.; Da Silva Santiago, A.; Santana, J.O.; De Sousa, A.O.; Alvim, F.C.; Pirovani, C.P. Proteomic Analysis during of Spore Germination of *Moniliophthora perniciosa*, the Causal Agent of Witches' Broom Disease in Cacao. *BMC Microbiol.* **2017**, *17*, 176. [CrossRef]
25. Mares, J.H.; Gramacho, K.P.; Santana, J.O.; Oliveira de Souza, A.; Alvim, F.C.; Pirovani, C.P. Hydrosoluble Phylloplane Components of Theobroma Cacao Modulate the Metabolism of *Moniliophthora perniciosa* Spores during Germination. *Fungal Biol.* **2020**, *124*, 73–81. [CrossRef]
26. dos Santos, E.C.; Pirovani, C.P.; Correa, S.C.; Micheli, F.; Gramacho, K.P. The Pathogen *Moniliophthora perniciosa* Promotes Differential Proteomic Modulation of Cacao Genotypes with Contrasting Resistance to Witches' Broom Disease. *BMC Plant Biol.* **2020**, *20*, 1. [CrossRef]
27. Fernández, M.B.; Pagano, M.R.; Daleo, G.R.; Guevara, M.G. Hydrophobic proteins secreted into the apoplast may contribute to resistance against *Phytophthora infestans* in potato. *Plant Physiol. Biochem.* **2012**, *60*, 59–66. [CrossRef]
28. Ali, S.S.; Melnick, R.L.; Crozier, J.; Phillips-Mora, W.; Strem, M.D.; Shao, J.; Zhang, D.; Sicher, R.; Meinhardt, L.; Bailey, B.A. Successful pod infections by *Moniliophthora roreri* result in differential *Theobroma cacao* gene expression depending on the clone's level of tolerance. *Mol. Plant Pathol.* **2014**, *15*, 698–710. Erratum in *Mol. Plant Pathol.* **2017**, *18*, 169. https://doi.org/10.1111/mpp.12498. [CrossRef]
29. Rincones, J.; Scarpari, L.M.; Carazzolle, M.F.; Mondego, J.M.; Formighieri, E.F.; Barau, J.G.; Costa, G.G.L.; Carraro, D.M.; Brentani, H.P.; Vilas-Boas, L.A.; et al. Differential gene expression between the biotrophic-like and saprotrophic mycelia of the witches' broom pathogen *Moniliophthora perniciosa*. *Mol. Plant-Microbe Interact.* **2008**, *21*, 891–908. [CrossRef] [PubMed]
30. Dias, C.V.; Mendes, J.S.; dos Santos, A.C.; Pirovani, C.P.; da Silva Gesteira, A.; Micheli, F.; Gramacho, K.P.; Hammerstone, J.; Mazzafera, P.; de Mattos Cascardo, J.C. Hydrogen Peroxide Formation in Cacao Tissues Infected by the Hemibiotrophic Fungus *Moniliophthora perniciosa*. *Plant Physiol. Biochem.* **2011**, *49*, 917–922. [CrossRef]
31. Camillo, L.R.; Filadelfo, C.R.; Monzani, P.S.; Corrêa, R.X.; Gramacho, K.P.; Micheli, F.; Pirovani, C.P. Tc-CAPX, a Cytosolic Ascorbate Peroxidase of *Theobroma cacao* L. Engaged in the Interaction with *Moniliophthora perniciosa*, the Causing Agent of Witches' Broom Disease. *Plant Physiol. Biochem.* **2013**, *73*, 254–265. [CrossRef] [PubMed]
32. Lim, D.; Hains, P.; Walsh, B.; Bergquist, P.; Nevalainen, H. Proteins associated with the cell envelope of *Trichoderma reesei*: A proteomic approach. *Proteom. Int. Ed.* **2001**, *1*, 899–910. [CrossRef]
33. Pitarch, A.; Sánchez, M.; Nombela, C.; Gil, C. Sequential fractionation and two-dimensional gel analysis unravels the complexity of the dimorphic fungus *Candida albicans* cell wall proteome. *Mol. Cell. Proteom.* **2002**, *1*, 967–982. [CrossRef]
34. DelVecchio, V.G.; Connolly, J.P.; Alefantis, T.G.; Walz, A.; Quan, M.A.; Patra, G.; Ashton, J.M.; Whittington, J.T.; Chafin, R.D.; Liang, X.; et al. Proteomic profiling and identification of immunodominant spore antigens of *Bacillus anthracis*, *Bacillus cereus*, and *Bacillus thuringiensis*. *Appl. Environ. Microbiol.* **2006**, *72*, 6355–6363. [CrossRef]
35. Alloush, H.M.; López-Ribot, J.L.; Masten, B.J.; Chaffin, W.L. 3-Phosphoglycerate kinase: A glycolytic enzyme protein present in the cell wall of *Candida albicans*. *Microbiology* **1997**, *143*, 321–330. [CrossRef]
36. Doyle, S. Fungal proteomics: From identification to function. *FEMS Microbiol. Lett.* **2011**, *321*, 1–9. [CrossRef]
37. Eroles, P.; Sentandreu, M.; Elorza, M.V.; Sentandreu, R. The highly immunogenic enolase and Hsp70p are adventitious *Candida albicans* cell wall proteins. *Microbiology* **1997**, *143*, 313–320. [CrossRef] [PubMed]
38. Angiolella, L.; Facchin, M.; Stringaro, A.; Maras, B.; Simonetti, N.; Cassone, A. Identification of a glucan-associated enolase as a main cell wall protein of *Candida albicans* and an indirect target of lipopeptide antimycotics. *J. Infect. Dis.* **1996**, *173*, 684–690. [CrossRef] [PubMed]
39. Chaffin, W.L. Cell wall proteins of *Candida albicans*. *Microbiol. Mol. Biol. Rev. MMBR* **2008**, *72*, 495–544. [CrossRef] [PubMed]
40. Egea, L.; Aguilera, L.; Gimenez, R.; Sorolla, M.A.; Aguilar, J.; Badía, J.; Baldoma, L. Role of secreted glyceraldehyde-3-phosphate dehydrogenase in the infection mechanism of enterohemorrhagic and enteropathogenic *Escherichia coli*: Interaction of the extracellular enzyme with human plasminogen and fibrinogen. *Int. J. Biochem. Cell Biol.* **2007**, *39*, 1190–1203. [CrossRef]
41. Barbosa, M.S.; Báo, S.N.; Andreotti, P.F.; de Faria, F.P.; Felipe, M.S.S.; dos Santos Feitosa, L.; Mendes-Giannini, M.J.S.; de Almeida Soares, C.M. Glyceraldehyde-3-phosphate dehydrogenase of *Paracoccidioides brasiliensis* is a cell surface protein involved in fungal adhesion to extracellular matrix proteins and interaction with cells. *Infect. Immun.* **2006**, *74*, 382–389. [CrossRef]
42. Guo, Y.; Song, Y. Differential proteomic analysis of apoplastic proteins during initial phase of salt stress in rice. *Plant Physiol.* **2009**, *4*, 121–122. [CrossRef]
43. Loguercio-Leite, C.; Dreschler-Santos, E.R.; Abrão, R.L. A particularidade de ser um fungo—I. Constituintes celulares. *Biotemas* **2006**, *19*, 17–27.
44. Cowen, L.E.; Steinbach, W.J. Stress, drugs, and evolution: The role of cellular signaling in fungal drug resistance. *Eukaryot. Cell* **2008**, *7*, 747–764. [CrossRef]
45. Henderson, A.; Hershey, J.W. Eukaryotic translation initiation factor (eIF) 5A stimulates protein synthesis in *Saccharomyces cerevisiae*. *Proc. Natl. Acad. Sci. USA* **2011**, *108*, 6415–6419. [CrossRef]

46. Wang, W.; Vinocur, B.; Shoseyov, O.; Altman, A. Role of plant heat-shock proteins and molecular chaperones in the abiotic stress response. *Trends Plant Sci.* **2004**, *9*, 244–252. [CrossRef]
47. Mogk, A.; Ruger-Herreros, C.; Bukau, B. Cellular functions and mechanisms of action of small heat shock proteins. *Annu. Rev. Microbiol.* **2019**, *73*, 89–110. [CrossRef]
48. Cooper, B.; Garrett, W.; Campbell, K. Shotgun identification of proteins from uredospores of the bean rust *Uromyces appendiculatus*. *Proteomics* **2006**, *6*, 2477–2484. [CrossRef] [PubMed]
49. Chandler, J.M.; Treece, E.R.; Trenary, H.R.; Brenneman, J.L.; Flickner, T.J.; Frommelt, J.L.; Oo, Z.M.; Patterson, M.M.; Rundle, W.T.; Valle, O.V.; et al. Protein profiling of the dimorphic, pathogenic fungus, *Penicillium marneffei*. *Proteome Sci.* **2008**, *6*, 17. [CrossRef]
50. Schmidt-Dannert, C. Biosynthesis of terpenoid natural products in fungi. *Biotechnol. Isoprenoids* **2015**, *148*, 19–61. [CrossRef]
51. Syed, K.; Shale, K.; Pagadala, N.S.; Tuszynski, J. Systematic identification and evolutionary analysis of catalytically versatile cytochrome p450 monooxygenase families enriched in model basidiomycete fungi. *PLoS ONE* **2014**, *9*, e86683. [CrossRef] [PubMed]
52. González-Fernández, R.; Prats, E.; Jorrín-Novo, J.V. Proteomics of plant pathogenic fungi. *J. Biomed. Biotechnol.* **2010**, *2010*, 932527. [CrossRef]
53. Roberts, M.R.; Salinas, J.; Collinge, D.B. 14-3-3 proteins and the response to abiotic and biotic stress. *Plant Mol. Biol.* **2002**, *50*, 1031–1039. [CrossRef]
54. Van Heusden, G.P.H. 14-3-3 Proteins: Insights from genome-wide studies in yeast. *Genomics* **2009**, *94*, 287–293. [CrossRef]
55. Würtele, M.; Jelich-Ottmann, C.; Wittinghofer, A.; Oecking, C. Structural view of a fungal toxin acting on a 14-3-3 regulatory complex. *EMBO J.* **2003**, *22*, 987–994. [CrossRef]
56. Chen, M.; Jiang, M.; Shang, J.; Lan, X.; Yang, F.; Huang, J.; Nuss, D.L.; Chen, B. CYP1, a hypovirus-regulated cyclophilin, is required for virulence in the chestnut blight fungus. *Mol. Plant Pathol.* **2011**, *12*, 239–246. [CrossRef] [PubMed]
57. Kim, I.S.; Kim, H.Y.; Shin, S.Y.; Kim, Y.S.; Lee, D.H.; Park, K.M.; Yoon, H.S. A cyclophilin A CPR1 overexpression enhances stress acquisition in *Saccharomyces cerevisiae*. *Mol. Cells* **2010**, *29*, 567–574. [CrossRef] [PubMed]
58. Monzani, P.S.; Pereira, H.M.; Gramacho, K.P.; Alvim, F.C.; Meirelles, F.V. Structural Analysis of Cyclophilin and Inhibitory Activity of Cyclosporin A on Germination and Growth of *Moniliophthora perniciosa*. *Pharm. Anal. Acta* **2011**, *S7*, 001. [CrossRef]
59. Pires, A.B.; Gramacho, K.P.; Silva, D.C.; Góes-Neto, A.; Silva, M.M.; Muniz-Sobrinho, J.S.; Porto, R.F.; Villela-Dias, C.; Brendel, M.; Cascardo, J.C.; et al. Early development of *Moniliophthora perniciosa* basidiomata and developmentally regulated genes. *BMC Microbiol.* **2009**, *9*, 158. [CrossRef] [PubMed]
60. Teixeira, P.J.P.L.; de Thomazella, D.P.T.; Reis, O.; do Prado, P.F.V.; do Rio, M.C.S.; Fiorin, G.L.; José, J.; Costa, G.G.L.; Negri, V.A.; Mondego, J.M.C.; et al. High-Resolution Transcript Profiling of the Atypical Biotrophic Interaction between Theobroma Cacao and the Fungal Pathogen *Moniliophthora Perniciosa*. *Plant Cell* **2014**, *26*, 4245–4269. [CrossRef]
61. Barbosa, C.S.; da Fonseca, R.R.; Batista, T.M.; Barreto, M.A.; Argolo, C.S.; de Carvalho, M.R.; do Amaral, D.O.J.; de Silva, E.M.A.; Arévalo-Gardini, E.; Hidalgo, K.S.; et al. Genome Sequence and Effectorome of *Moniliophthora perniciosa* and *Moniliophthora roreri* Subpopulations. *BMC Genom.* **2018**, *19*, 509. [CrossRef]
62. Pierre, S.; Griffith, G.W.; Morphew, R.M.; Mur, L.A.J.; Scott, I.M. Saprotrophic Proteomes of Biotypes of the Witches' Broom Pathogen *Moniliophthora perniciosa*. *Fungal Biol.* **2017**, *121*, 743–753. [CrossRef]
63. Mondego, J.M.; Carazzolle, M.F.; Costa, G.G.; Formighieri, E.F.; Parizzi, L.P.; Rincones, J.; Cotomacci, C.; Carraro, D.M.; Cunha, A.F.; Carrer, H.; et al. A Genome Survey of *Moniliophthora perniciosa* Gives New Insights into Witches' Broom Disease of Cacao. *BMC Genom.* **2008**, *9*, 548. [CrossRef]
64. Morin, E.; Kohler, A.; Baker, A.R.; Foulongne-Oriol, M.; Lombard, V.; Nagye, L.G.; Ohm, R.A.; Patyshakuliyeva, A.; Brun, A.; Aerts, A.L.; et al. Genome sequence of the button mushroom *Agaricus bisporus* reveals mechanisms governing adaptation to a humic-rich ecological niche. *Proc. Natl. Acad. Sci. USA* **2012**, *109*, 17501–17506. Erratum in *Proc. Natl. Acad. Sci. USA* **2013**, *110*, 4146. [CrossRef] [PubMed]
65. Jumper, J.; Evans, R.; Pritzel, A.; Green, T.; Figurnov, M.; Ronneberger, O.; Tunyasuvunakool, K.; Bates, R.; Žídek, A.; Potapenko, A.; et al. Highly accurate protein structure prediction with AlphaFold. *Nature* **2021**, *596*, 583–589. [CrossRef]
66. Blum, M.; Chang, H.-Y.; Chuguransky, S.; Grego, T.; Kandasaamy, S.; Mitchell, A.; Nuka, G.; Paysan-Lafosse, T.; Qureshi, M.; Raj, S.; et al. The InterPro protein families and domains database: 20 years on. *Nucleic Acids Res.* **2021**, *49*, D344–D354. [CrossRef]
67. Wang, J.; Li, M.; Chen, J.; Pan, Y. A fast hierarchical clustering algorithm for functional modules discovery in protein interaction networks. *IEEE/ACM Trans. Comput. Biol. Bioinform.* **2010**, *8*, 607–620. [CrossRef] [PubMed]
68. Spirin, V.; Mirny, L.A. Protein complexes and functional modules in molecular networks. *Proc. Natl. Acad. Sci. USA* **2003**, *100*, 12123–12128. [CrossRef] [PubMed]
69. Gramacho, K.P.; Pires, J.L.; Clément, D.; Juca, F.F.; Melo, G.R.; Patrocinio, N.G.R.B.; Moreira, R.F.; Sousa, L.A.; Lopes, U.V. Breakdown of scavina resistance in Bahia caused by the evolution. In Proceedings of the 17th Conférence Internationale sur la Recherche Cacaoyère, Yaounde, Cameroun, 15–20 October 2012.

70. Santos, F.F.J.; Pires, J.L.; Lopes, U.V.; de Brito, L.A.S.; Filho, L.P.d.S.; Lemos, L.S.L.; Gramacho, K.P. Mycelial Growth, Starch Degradation Ability and Aggressiveness of *Moniliophthora perniciosa* Isolates towards Cacao. *Trop. Plant Pathol.* **2017**, *42*, 21–27. [CrossRef]
71. Gramacho, I.C.P.; Magno, A.E.S.; Mandarino, E.P.; Matos, A. *Cultivo e Beneficiamento do Cacau na Bahia*; CEPLAC/CEDEX: Ilhéus, Brazil, 1992.
72. Lopes, U.V.; Monteiro, W.R.; Pires, J.L.; Clement, D.; Yamada, M.M.; Gramacho, K.P. Cacao breeding in Bahia, Brazil—Strategies and results. *Crop Breed. Appl. Biotechnol.* **2001**, *11*, 73–81. [CrossRef]
73. Pirovani, C.P.; Carvalho, H.A.S.; MaChado, R.C.R.; Gomes, D.S.; Alvim, F.C.; Pomella, A.W.V.; Gramacho, K.P.; Cascardo, J.C.d.M.; Pereira, G.A.G.; Micheli, F. Protein extraction for proteome analysis from cacao leaves and meristems, organs infected by *Moniliophthora perniciosa*, the causal agent of the witches' broom disease. *Electrophoresis* **2008**, *29*, 2391–2401. [CrossRef] [PubMed]
74. Neuhoff, V.; Arold, N.; Taube, D.; Ehrhardt, W. Improved staining of proteins in polyacrylamide gels including isoelectric focusing gels with clear background at nanogram sensitivity using Coomassie Brilliant Blue G-250 and R-250. *Electrophoresis* **1988**, *9*, 255–262. [CrossRef]
75. Shevchenko, A.; Tomas, H.; Havli, J.; Olsen, J.V.; Mann, M. In-gel digestion for mass spectrometric characterization of proteins and proteomes. *Nat. Protoc.* **2006**, *1*, 2856–2860. [CrossRef]
76. de Oliveira, B.V.; Teixeira, G.S.; Reis, O.; Barau, J.G.; Teixeira, P.J.P.; do Rio, M.C.S.; Domingues, R.R.; Meinhardt, L.W.; Leme, A.F.P.; Rincones, J.; et al. A potential role for an extracellular methanol oxidase secreted by *Moniliophthora perniciosa* in Witches' broom disease in cacao. *Fungal Genet. Biol.* **2012**, *49*, 922–932. [CrossRef] [PubMed]
77. Mora-Ocampo, I.Y.; Pirovani, C.P.; Luz, E.D.; Rêgo, A.P.; Silva, E.M.; Rhodes-Valbuena, M.; Corrêa, R.X. *Ceratocystis cacaofunesta* differentially modulates the proteome in xylem-enriched tissue of cocoa genotypes with contrasting resistance to Ceratocystis wilt. *Planta* **2021**, *254*, 94. [CrossRef] [PubMed]